university of groningen

faculty of science and engineering

Symmetry Analysis of Non-Collinear Antiferromagnets

Author:
Sergiusz POLAK
(s5085225)

Supervisor:
prof. dr. Maxim MOSTOVOY
Supervisor:
prof. dr. Holger WAALKENS

Bachelor's Thesis
To fulfill the requirements for the degree of
Bachelor of Science in Physics
Bachelor of Science in Mathematics
at the University of Groningen

July 9, 2025

Contents

Abstract

Altermagnets, which are antiferromagnets exhibiting responses typical of ferromagnets, have recently emerged as a promising platform for spintronic devices. Spin groups are often used to analyze altermagnets, as unlike magnetic groups, they allow one to distinguish non-relativistic effects independent of spin-orbit coupling (SOC). In this study, the representation theory of spin point groups and magnetic point groups is used to analyze the occurrence of the anomalous Hall effect (AHE), $\mathcal{T}$-odd spin Hall effect (SHE), and spin-splitting of electron bands in selected non-collinear antiferromagnets Mn_3X (X = Ir, Ge, Sn) , Mn_3NiN, and $MnTe_2$. The allowed components of the tensors describing these effects are explicitly determined, both in the presence and absence of SOC. The study demonstrates a link between $\mathcal{T}$-odd SHE and spin splitting of bands quadratic in the wavevector $\vec{k}$. The calculations demonstrate that all of the analyzed materials permit SOC-free $\mathcal{T}$-odd spin Hall effect and quadratic spin splitting, while Mn_3X and Mn_3NiN allow AHE and a weak ferromagnetic moment with SOC. Furthermore, the study determines all the allowed components of the $\mathcal{T}$-odd spin conductivity tensor σ_{ij}^{α} with and without SOC, and by extension, the allowed quadratic spin-splitting terms, as well as enumerating the quartic and sextic spin-splitting terms with or without SOC for the analyzed materials. The results agree with the experiments and demonstrate the effectiveness of a basic representation theory approach.

Keywords: altermagnet, non-collinear antiferromagnet, spin group, spin Hall effect

1 Introduction

Magnetism has been known to humanity since at least the 6th century BCE, when the Greek philosopher Thales from Miletus tried to explain the unique properties of the naturally magnetized lodestones [1]. Lodestones belong to ferromagnets, materials characterized by their magnetizability and a strong attraction to magnets. Ferromagnets have found numerous uses - transformers, generators, hard drives, electromagnets, to name a few. Antiferromagnets cannot be magnetized, in this aspect akin to non-magnetic matter, and were discovered only around the year 1932 [2]. Together with ferromagnets, antiferromagnets make up the two traditional classes of magnetic crystals.

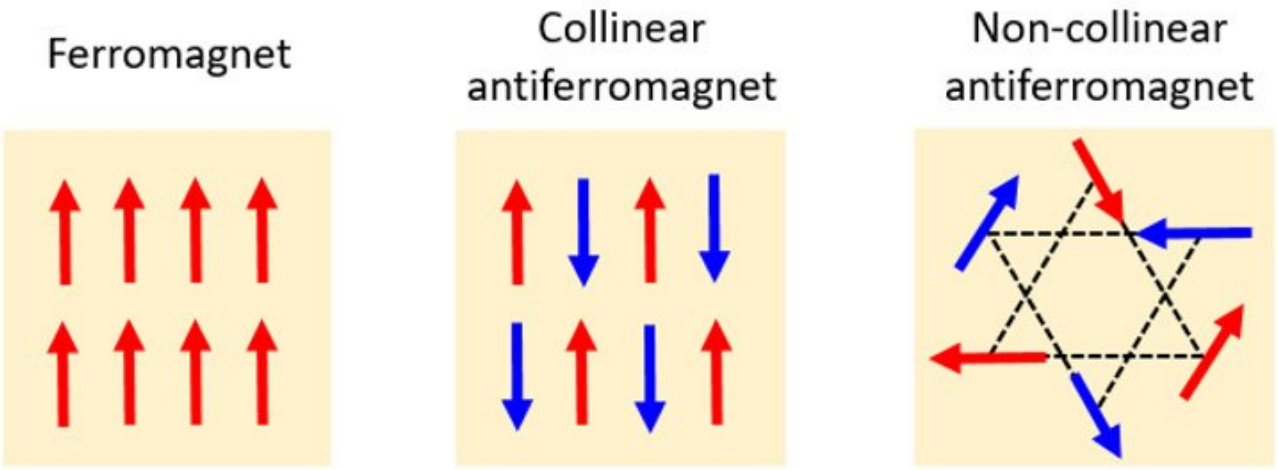

Figure 1: Magnetic ordering in ferromagnets and antiferromagnets ©Jiahao Han.

The properties of magnetic crystals result from magnetic ions, which have magnetic moments generated by their spins. In ferromagnets, the spins within the unit cell are aligned, leading to mesoscopic magnetic domains. The domains are randomly oriented in unmagnetised ferromagnets, but they can be aligned with an external magnetic field, leading to the generation of a macroscopic magnetic field. In antiferromagnets, the spins within the magnetic unit cell compensate. These materials also have domains, characterized by a particular orientation of the compensating spins, but contrary to ferromagnets, the antiferromagnetic domains generate a negligible magnetic field. Various arrangements can have compensating magnetic moments- collinear, triangular, tetrahedral, or spiral. Ferromagnetic, collinear antiferromagnetic, and triangular arrangements are displayed in Figure 1. This paper focuses on the less-studied non-collinear antiferromagnets.

Ferromagnets exhibit unique effects when interacting with electrons or photons; examples are the anomalous and spin Hall effects, the Faraday and inverse Faraday effect, and the spin-splitting of electron bands in conducting ferromagnets. These and other effects are being increasingly employed in spintronics applications. Spintronics, named after spin and electronics, aims to use electron spins for various functions [3]. Spintronics devices are predicted to be more efficient, and some spintronic technologies, such as MRAM, are in early stages of commercialization [4]. Spintronic systems are also potential platforms for quantum and neuromorphic computing [5].

It was thought that the magnitude of the anomalous Hall effect and similar responses is minuscule in antiferromagnets, which has limited the application of antiferromagnets in spintronics to coupled ferromagnet-antiferromagnet systems [6]. This view was challenged in 2014 in a paper by Chen et al. [7], which predicted large AHE (anomalous Hall effect) in non-collinear antiferromagnets. A year later, a study by Nakatsuji et al. [8] found large AHE in Mn_3Sn, while a 2016 study by Nayak et

al. experimentally verified highly anisotropic large anomalous and spin Hall effects in Mn_3Ge [9]. New studies also predict [10] [11] and verify [12] the presence of AHE in collinear antiferromagnets. There are also recent studies of spin-splitting of bands and spin textures in collinear [13] [14] and non-collinear [15] [16] antiferromagnets. The name altermagnets was coined to describe antiferromagnets exhibiting properties typical of ferromagnets. Various materials are predicted to be altermagnetic, covering the whole spectrum from insulators to conductors [13]. Such antiferromagnets, especially non-collinear AFMs (antiferromagnets) offer unique advantages for spintronics applications, such as lack of stray fields and higher stability in magnetic fields [6] [5] [17].
The unique properties of altermagnets cannot be solely attributed to their magnetic arrangement - the position of non-magnetic ions in the cell can determine whether the material will show spin splitting or not [18]. The properties arise from the breaking of certain symmetries by the magnetic order of the crystal. For example, the anomalous Hall effect requires the breaking of $\mathcal{T}$ inversion combined with the spatial $\mathcal{P}$ inversion and translations T. Symmetry analysis in antiferromagnets can be used to constrain effects such as the anomalous Hall effect (AHE) [13], spin Hall effect (SHE) [19], and spin-splitting [20] of bands. It can also be used to find band degeneracies [21].
A symmetry group consists of operations that leave the system indistinguishable and conserve its energy [22]. While symmetries of an ordinary crystal are described using point and space groups, the symmetries of a magnetic material are usually described using magnetic groups, which contain combinations of (improper) rotations, translations, and T-inversion. These elements are spacetime isometries, and they conserve all relativistic effects, such as spin-orbit coupling (SO coupling). Spin groups, on the other hand, allow for more operations than magnetic groups. The elements of a spin space group allow for partially decoupled spin and spatial rotations, which break SO coupling. These new operations are approximate symmetries for materials with low SO coupling, which are relatively abundant [21]. Materials with high SO coupling contain high-Z elements, which are often expensive or toxic [18]. If an effect is allowed by the spin space group, it is independent of the SO coupling; thus, it can be of much larger magnitude. Spin groups were first invented in 1966 [23], and all 655 spin point groups were determined in 1974 [24]. The formalism was used sparsely, but recently the interest in it has resurfaced. Spin space groups were classified by three independent research groups in 2024 [25] [20] [26], and in 2023 a Python library for determining the spin space group (ssg) of a magnetic material, used in this paper, was published [27]. Spin groups and their representations can be used to analyze extra band degeneracies [25] [21], and to analyze the existence of various effects in antiferromagnets [13] [14] [19] [18].
Representation theory is a tool often used in symmetry analysis. Various physical concepts can be expressed in terms of scalars, vectors, or tensors, which all belong to a vector space. The symmetry elements act on the vector space, and in the simplest case, they form a representation - the group elements can be embedded as invertible matrices that respect the group law, i.e.

$$[g * h] = [g][h] \tag{1}$$

where $g, h \in G$, G is the symmetry group, and $[g]$ is the representation of the element g as a matrix. There also exist projective representations and corepresentations, which are useful in the study of the band structures [25] [20] [26]. The representation of a group, being a matrix, acts on a certain carrier vector space. The carrier space, together with the representation acting on it, forms an ($\mathbb{F}G$) module[28]. Modules can contain submodules - subspaces that are closed under group action. By definition, the action of the group elements maps the elements of a submodule back to itself. By decomposing representations and modules into subrepresentations and submodules, one can separate the components of a tensor based on how they transform under the symmetry group, and find the ones that do not transform at all - the invariant components. This can also be found by finding the genera-

tors of the group and examining how the tensor components transform under their action. Symmetries are also connected to the order parameters that govern phase transitions. In Landau's theory of phase transitions, a nonzero value of an order parameter signals the breaking of the symmetries of a high-entropy state. During a phase transition from a high-entropy to a low-entropy state, the equilibrium value of an order parameter becomes nonzero [29].

1.1 Research questions and the scope of the project.

The scope of this paper is to characterize and constrain various effects in candidate altermagnets based on symmetry analysis. The analysed materials are Mn_3Ir, Mn_3Ge, Mn_3Sn, Mn_3NiN, and $MnTe_2$, which show or are theoretically predicted to show AHE, SHE [9] [8] [7] [30] or spin splitting [16] [15]. The analysis can be easily extended to other translation-symmetry conserving antiferromagnets, and possibly beyond.

The following effects will be analyzed, each of them described by a tensor:

1. Weak magnetic moment, anomalous Hall effect, Faraday rotation - effects described by a T-odd axial vector, for example, Hall conductivity $\vec{\sigma}_H$.

2. Spin texture in the momentum space, described by the expectance of spin at a given $\vec{k}$, written as $\langle \hat{S} \rangle (\vec{k})$.

3. Electrical generation of spin-current and T-odd spin Hall effect, described by rank 3 tensor σ_{ij}^{α} or a rank 2 pseudotensor σ_{i}^{α} for the SHE (spin Hall effect).

All of these effects are important for spintronics applications. For instance, a weak magnetic moment allows for the selection of antiferromagnetic domains, and spin polarization of the electronic bands can be used to convert an electric current into a spin current [31].
The effect tensors will be analyzed using representation theory. Each tensor transforms under a representation of the spin point group of the material, and the space of the tensors forms a module. By determining its trivial submodules, the basis of the subspace of the symmetry-allowed tensors is determined. The dimension of this subspace can be calculated independently to ensure that the full basis of the symmetry-allowed subspace is found.
The project aims to use basic representation theory to study the unique properties of altermagnets.

2 Theory and the background literature

2.1 Representation theory.

This subsection is based on the second edition of *Representations and Characters of Groups* by J. Gordon and M. Liebeck [28].
A representation of a group is a homomorphism from the group G into the group $GL(n,\mathbb{F})$ of invertible $n \times n$ matrices over a field. The integer n is the degree of the representation.

$$\begin{aligned} &[\cdot] : G \to GL(n,\mathbb{F}) \\ &[g*h] = [g][h] \end{aligned} \tag{2}$$

Two representations $[\cdot]_A$ and $[\cdot]_B$ of the same degree are considered equivalent if there is an invertible matrix T such that $[\cdot]_A = T[\cdot]T^{-1}$. The representation acts on the vector space $\mathbb{F}^n$, and the vector space together with the representation is a $\mathbb{F}G$-module. Formally, a $\mathbb{F}G$ module is a vector space V over $\mathbb{F}$ with a linear and associative group action

$$\begin{aligned} &g(\lambda\vec{u}+\mu\vec{v}) = \lambda g\vec{u}+\mu g\vec{v} \\ &g(h(\vec{v})) = (gh)\vec{v} \end{aligned} \tag{3}$$

for all $\vec{u},\vec{v} \in V$, $\lambda,\mu \in \mathbb{F}$, $g,h \in G$.
The action of G on a module V is extended to the action of $\mathbb{F}G$, the vector space (and a module) of linear combinations $\lambda g+\mu h$ of the elements g,h of G, in the following way

$$(\lambda g+\mu h)\vec{v} = \lambda g\vec{v}+\mu h\vec{v} \tag{4}$$

where $\vec{v} \in V$, $\lambda,\mu \in \mathbb{F}$, $g,h \in G$
Different bases of a $\mathbb{F}G$ module correspond to different equivalent representations of a group, such that an $\mathbb{F}G$ module is a description of a representation and the collection of all representations equivalent to it, corresponding to different bases of the module. One can define an (isomorphism) homomorphism ϕ between $\mathbb{F}G$-modules U and V as a (bijective) linear transformation which is compatible with the group action, i.e.

$$\varphi : U \to V \tag{5}$$
$$\varphi(\lambda\vec{u}+\mu\vec{v}) = \lambda\varphi(\vec{u})+\mu\varphi(\vec{v}) \tag{6}$$
$$g\varphi(\vec{u}) = \varphi(g\vec{u}) \tag{7}$$

for $\vec{u},\vec{v} \in U$, $\lambda,\mu \in \mathbb{F}$, $g \in G$.
By the construction of the action of $\mathbb{F}G$ on $\mathbb{F}G$ modules, a $\mathbb{F}G$ module homomorphism $\phi : U \to V$ between $\mathbb{F}G$ modules U,V is also compatible with the action of $\mathbb{F}G$

$$\phi(r\vec{u}) = r\phi(\vec{u}) \tag{8}$$

where $r \in \mathbb{F}G$, $\vec{u} \in U$.
In this paper, all modules will be $\mathbb{C}G$ modules over finite groups.
A submodule U of a module V is a subspace of V that is also a module, i.e., U is closed under the group action. An irreducible module V is a module that does not have a nontrivial submodule (not equal to $\{0\}$ or V). As a vector space of one dimension only has subspaces of dimensions 0 and 1, every 1 one-dimensional $\mathbb{F}G$ module is irreducible.

With the previous assumption, by Maschke's Theorem [28], if U is a submodule of V, there exists a submodule W of V such that V is a direct sum of U and W.

$$V = U \oplus W \tag{9}$$

Every non-irreducible module, by definition, has a nontrivial submodule. Because of this, by using induction on the dimension of the module in conjunction with the above result, a finite-dimensional $\mathbb{C}G$ module of a finite group can be decomposed as a direct sum of irreducible submodules. This can be equivalently expressed as every complex representation of a finite group being block-diagonalizable. Each module can be decomposed into a sum of irreducible modules, and a finite group allows for finitely many non-isomorphic irreducible $\mathbb{C}G$ modules.

A character χ of a representation $[\cdot]$is a mapping of a group element to the trace of its representation matrix, $\chi(g) = Tr([g])$. Because $Tr(AB) = Tr(BA)$ for complex matrices, $Tr(T[\cdot]T^{-1}) = Tr([\cdot])$, i.e. equivalent representations have the same character. This allows for ascribing a character to a module by choosing the character of any associated representation.

By the orthogonality theorem, for irreducible $\mathbb{C}G$ modules U_i, U_j of a finite group, where $i = j \iff U_i \cong U_j$, the associated characters χ_i, χ_j are orthonormal, i.e.

$$\langle \chi_i, \chi_j \rangle = \frac{1}{|G|} \sum_{g \in G} \overline{\chi}_i(g) \chi_j(g) = \delta_{ij}. \tag{10}$$

If a module V decomposes into

$$\bigoplus_{i=1}^{k} d_i U_i$$

then $\langle \chi_V, \chi_i \rangle = d_i$.

Finally, if U is an irreducible $\mathbb{C}G$ module and χ is the associated character, the element of $\mathbb{C}G$ given by

$$1_U = \frac{1}{|G|} \sum_{g \in G} \overline{\chi}(g) g \tag{11}$$

when applied to a $\mathbb{C}G$ module V projects V onto the sum of its submodules $\bigoplus U_i$ which are isomorphic to U [28]. From the theory of linear algebra, all $\vec{v} \in V$ can be uniquely decomposed as $\vec{v} = \vec{u} + \vec{w}$, where $\vec{u} \in \bigoplus U_i$ and $\vec{w} \in V - \bigoplus U_i$ or $\vec{w} = \vec{0}$. The operator 1_U acts on $\vec{v} = \vec{u} + \vec{w}$ in the following way:

$$1_U(\vec{u} + \vec{w}) = \vec{u} \tag{12}$$

for $\vec{u}, \vec{w}$ defined as before. Equivalently,

$$1_U(\vec{v}) = \vec{v} \iff \vec{v} \in \bigoplus U_i \tag{13}$$

for $\vec{v} \in V$, i.e. the elements of $\bigoplus U_i$ are precisely the eigenvectors of 1_U which are associated with the eigenvalue $\lambda = 1$. By solving the eigenvalue problem for the projection operator 1_U and selecting the eigenvectors corresponding to the eigenvalue $\lambda = 1$, one finds the complete basis of $\bigoplus U_i$, the direct sum of the submodules U_i of a $\mathbb{C}G$ module V which are isomorphic to an irreducible $\mathbb{C}G$ module U.

The application projection operator 1_U on $\vec{v} \in V$ can be interpreted as an average of all possible images $g\vec{v}$ of $\vec{v}$ under the group action by $g \in G$, weighted with the character χ_U.

2.2 Magnetic groups and spin groups.

This subsection is based on two papers. First is a 1974 paper by D.B Litvin and W. Opechowski [24], which formalized spin groups and classified 655 (now agreed to be 598) inequivalent spin point groups. The second is the classification of spin space groups by Chen et al. [20], completed in 2024, in parallel with two other groups [25] [26].
Individual spins within the magnetic crystal cell are quantum mechanical objects and exist in a superposition of directions. A definite spin direction emerges only as an average over many crystal cells [32]. This average spin can be approximately treated as a vector in $\mathbb{R}^3$, attributed to each magnetic ion in the lattice, as in Figure 2.

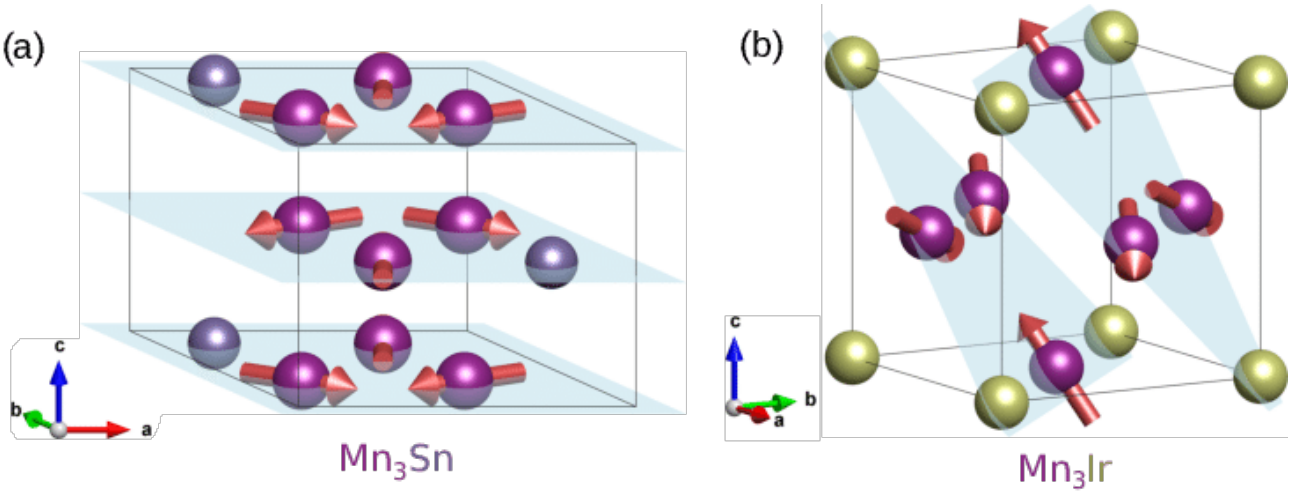

Figure 2: Magnetic arrangement of a) Mn_3Sn and b) Mn_3Ir, from [19].

A magnetic arrangement on a crystal is given by a function $\vec{M}(\vec{r}_i)$ from $\mathbb{R}^3$ to $\mathbb{R}^3$ defined on magnetic sites $\vec{r}_i$ within a magnetic cell, which might encompass many crystal cells. This function maps the positions of the magnetic ions to their average magnetic moment, and can be constructed from experimental data. Positions within the magnetic cell are often expressed in the crystal coordinate system, which uses the cell's base vectors $\vec{a}$, $\vec{b}$, $\vec{c}$ as basis. The symmetry operations of a magnetic crystal keep the crystal, as well as its magnetic arrangement, invariant. A magnetic space group (MSG) $\mathcal{G}_M$ is the set of spacetime operations that conserve the magnetic arrangement. The operations are given by $\mathcal{T}^a\{R|\vec{v}\}$, where $a \in \{0,1\}$, $\mathcal{T}$ is the time-inversion, $R \in O(3)$ is a rotation or an improper rotation, and $\vec{v} \in \mathbb{R}^3$ is a translation. An operation $\mathcal{T}^a\{R|\vec{v}\}$ acts on the magnetic arrangement as follows:

$$\vec{M}(\vec{r}_i) \mapsto (-1)^a det(R) R\vec{M}(R^{-1}\vec{r}_i - R^{-1}\vec{v}) \tag{14}$$

A magnetic moment acts as an axial vector under rotation R, is possibly inverted by $\mathcal{T}$, and the sites $\vec{r}_i$ are interchanged by $\{R|\vec{v}\}^{-1}$.The magnetic point group P_M is defined by the set of $\mathcal{T}^a R$ such that $\mathcal{T}^a\{R|\vec{v}\} \in \mathcal{G}_M$. Magnetic point groups are finite.
A spin space group allows for partially decoupled spin and spatial rotations, and separates magnetic (spin) vectors and spatial vectors or axial vectors. Formally, the spin space group (SSG) $\mathcal{G}_S$ is given by the set of $\{S\|R|\vec{v}\}$ leaving the magnetic arrangement invariant. $R \in O(3)$ is a spatial (improper) rotation, $\vec{v} \in \mathbb{R}^3$ is a translation, and $S \in O(3)$ is the spin rotation, with improper rotations encoding $\mathcal{T}$-inversions. The spin rotation S only acts on spin vectors, such as magnetic moments, leaving spatial vectors invariant. Similarly, the spatial rotation or an improper rotation R and translations by a vector

$\vec{v}$ act on spatial vectors, and not spin vectors. An element $\{S\|R|\vec{v}\}$ of the SSG acts on the magnetic arrangement as follows:

$$\vec{M}(\vec{r}_i) \mapsto S\vec{M}(R^{-1}\vec{r}_i - R^{-1}\vec{v}) \tag{15}$$

where the S rotation rotates the magnetic moments, while the spatial isometry $\{R|\vec{v}\}$ interchanges the lattice sites.

By construction, spin space groups are supergroups of magnetic space groups, and the new allowed operations break SOC. Because of this, spin groups are descriptions of approximate symmetries in low SOC materials. There is a slight inconsistency, as a definite magnetic arrangement is only possible with SOC, as without SOC, different magnetic arrangements related by a spin rotation S would have the same energy. This problem is solved by assuming the experimentally determined magnetic order. An effect allowed by the spin space group is approximately independent of SOC, only requiring small, non-zero SOC, which is necessary to fix the magnetic arrangement. This is what is meant by SOC-free in this paper.

There is an equivalent method for the construction of SSG, by using XU instead of S for spin operations, where $X \in \{E, \mathcal{T}\}$, $U \in SU(2)$. This definition of SSG is equivalent as $SU(2)$ double covers $SO(3)$, and $O(3) \cong SO(3) \times \{E, \mathcal{T}\}$. This approach was used by Xiao et al. [25].

Spin space groups can be factored into a spin-only part and a nontrivial part.

$$\mathcal{G}_S = G_{SO} \times G_{NT} \tag{16}$$

G_{SO} contains elements $\{S||E|\vec{0}\}$, and has 4 possible types - nonmagnetic, collinear, coplanar, and non-coplanar. For a nonmagnetic arrangement, $G_{SO} = O(3)$. For a collinear arrangement, G_{SO} contains all rotations around the moment axis, and all the mirror symmetries containing this axis. If Z_2 is one such mirror, $G_{SO} \cong SO(2) \rtimes \{E, Z_2\}$, and the spin only group is infinite[20]. For a coplanar arrangement, the spin-only group contains the identity and the plane-mirror Z_2: $G_{SO} = \{E, Z_2\}$. In the non-coplanar case, G_{SO} is trivial.

The nontrivial ssg G_{NT} can be projected onto a *family group* $\mathcal{F}$, which is given by the set of $\{R|\vec{v}\}$ such that $\{S\|R|\vec{v}\} \in G_{NT}$. The family group is a subgroup of the paramagnetic phase's space group.G_{NT} also contains the spatial subgroup L, which is the set of $\{R, \vec{v}\}$ such that $\{E||R|\vec{v}\} \in G_{NT}$.

The group G_{NT} can be written as a coset decomposition.

$$G_{NT} = L + \{S_1, R_1\}L + \cdots + \{S_k, R_k\}L \tag{17}$$

It can be shown that L is a normal subgroup of G_{NT}: it is the kernel of the projection homomorphism from G_{NT} to $O(3)$.

$$\begin{aligned} G_{NT} &\to O(3) \\ \{S\|R|\vec{v}\} &\mapsto S \end{aligned} \tag{18}$$

Litvin et al. show that $L \lhd \mathcal{F}$, and that $\mathcal{F}/L \cong G/L$. In the analyzed materials, translation symmetry is not broken, and the translation subgroup of $\mathcal{F}$ is in L, so that $\mathcal{F}/L$ is a crystallographic point group. Spin point group is given by $P_S = \{\{S\|R\} \mid \{S\|R|\vec{v}\} \in \mathcal{G}_S \text{ for some } \vec{v}\}$, analogously to the magnetic point groups. The materials analyzed in this paper are non-collinear and have unbroken translation symmetry, so the corresponding spin point groups are finite.

When acting on the electron Bloch wavefunctions, the time reversal $\mathcal{T}$ is an antilinear operator, for $z \in \mathbb{C}$ satisfying the following.

$$\mathcal{T}(\psi_1 + \psi_2) = \mathcal{T}\psi_1 + \mathcal{T}\psi_2 \tag{19}$$

$$\mathcal{T}(z\psi) = \bar{z}\mathcal{T}\psi \tag{20}$$

To accommodate for the antilinearity of the $\mathcal{T}$ operator, the theory of corepresentations needs to be used when working with the Bloch basis [20]. In some applications, projective representation or corepresentations are used, which allow for additional phase factors. In this project, the analyzed tensors are real, so the $\mathcal{T}$ acts as a linear operator. Because of this, the simpler representation theory can be used instead of corepresentation theory.

2.3 Description of the individual effects.

2.3.1 Anomalous Hall effect.

An anomalous Hall effect (AHE) is the generation of an electrical current (or voltage) perpendicular to the applied electric field in magnetic structures. AHE dates back to 1881, two years after the discovery of the analogous ordinary Hall effect [33], but the origin of these effects is different. The ordinary Hall effect involves an external magnetic field that generates a Lorentz force on the charge carriers. The anomalous Hall effect, on the other hand, is caused by extrinsic scattering from magnetic impurities, or from the intrinsic nonzero integral of the Berry curvature over the occupied electron states [33]. The effect was traditionally studied in ferromagnets, but the new theoretical, computational [7] [10] [11] and experimental [8] [9] [12] work demonstrates strong AHE in select antiferromagnets. AHE can be described by the Hall conductivity axial vector $\vec{\sigma}_H$ [33].

$$\vec{J} = \vec{\sigma}_H \times \vec{E} \tag{21}$$

The nonzero anomalous Hall effect requires the breaking of $\mathcal{T}$-symmetry and the breaking of $\mathcal{T}$-symmetry composed with $\mathcal{P}$-inversion or a translation. In collinear and coplanar antiferromagnets, it also requires SOC, while noncoplanar arrangements can induce the topological Hall effect, which does not require SOC [22] [10]. By the Onsager reciprocity relations, the axial vector $\vec{g}(\omega)$ describing Faraday and Kerr effects is $\mathcal{T}$-odd, and it transforms in the same way as $\vec{\sigma}_H$ under magnetic and spin symmetry operations [31] [22], which results in these vectors having the same allowed components. This does not imply that the magnitudes of these components are connected; they only need to share the same allowed directions.

2.3.2 Weak ferromagnetic moment.

Some antiferromagnets exhibit a weak ferromagnetic moment, resulting from the imperfect cancellation of the individual magnetic moments, canting. This weak ferromagnetic moment, WFM in short, is orders of magnitude smaller than in ferromagnets or ferrimagnets. As an example, the magnetic moment of Mn_3Ge is around 0.007 μ_B [34] per Mn atom, compared to 1 μ_B per Mn in the ferrimagnet $Mn_5Si_3C_{1.5}$. WFM originates weak relativistic interactions such as Dzyaloshinskii-Moriya interactions [35]. Under the magnetic point group, the magnetic moment $\vec{M}$ transforms as a $\mathcal{T}$-odd axial vector, same as $\vec{\sigma}$. Under the spin point group, $\vec{M}$ transforms under spin rotations, while $\vec{\sigma}$ transforms under proper spatial rotations and time inversion. Magnetic moment is given by:

$$M_i = \frac{\partial f}{\partial H_i} \tag{22}$$

Where f is the free energy density and $\vec{H}$ is the magnetic field [31]. The free energy density transforms as a scalar, and it is invariant under all crystal symmetries and spatial isometries in general. This includes the $\mathcal{T}$-reversal symmetry.

2.3.3 Spin conductivity and $\mathcal{T}$-odd spin Hall effect.

Spin conductivity refers to the generation of a spin current J_i^α density by an applied electric field $\vec{E}$. As ordinary currents are related to the electric field by the conductivity tensor σ_{ij}, nonzero spin conductivity allows for conversion of a charge current into a spin current. $\mathcal{T}$-odd Spin Hall effect involves the generation of a spin current transverse to the applied electric current or electric field. SHE can be divided into ordinary SHE, generated by applying a magnetic field, or anomalous SHE originating from magnetic order [36]. A spin current is the transport of a spin component in a specific direction, just as an electronic current is the transport of electronic charge in a specific direction. The spin current density is described by a second-order tensor, where J_i^α corresponds to the current density of the spin component α in the direction i. SHE is governed by the antisymmetric part of the third-order spin-conductivity tensor σ_{ij}^α:

$$J_i^\alpha = \sigma_{ij}^\alpha E_j \tag{23}$$

The equation above uses the Einstein summation convention, where repeated indices are summed over.
A second-order antisymmetric tensor in 3 dimensions is dual to an axial vector [31], resulting in the following equation.

$$\vec{J^\alpha} = \vec{\sigma}^\alpha \times \vec{E} \tag{24}$$

Then σ_i^α is a second-order pseudotensor, which is $\mathcal{T}$-odd. The spin current J_i^α is $\mathcal{T}$-even, so the $\mathcal{T}$-odd SHE equation (24) is not $\mathcal{T}$-covariant, and the generated spin current is dissipative. This is also true for the $\mathcal{T}$-odd spin conductivity equation (23).

2.3.4 Spin polarization of bands.

In non-collinear antiferromagnets, spin polarization of bands can be expressed as $\langle\hat{S}\rangle(\vec{k})$, the expectation value of the spin operator at a wavevector $\vec{k}$ in the Brillouin zone. This spin vector transforms under the little group at $\vec{k}$, which only contains the symmetry elements keeping $\vec{k}$ invariant. One can also perform the expansion of $\langle\hat{S}\rangle(\vec{k})$ near some $\vec{k_0}$, for example $\vec{k} = \vec{0}$. The expansion near $\vec{k}_0 = \vec{0}$ is given by:

$$\langle\hat{S}\rangle_\alpha(\vec{k}) = \langle\hat{S}\rangle_\alpha(0) + \frac{\partial\langle\hat{S}\rangle_\alpha}{\partial\vec{k}}|_{\vec{0}} \cdot \vec{k} + \frac{1}{2}\vec{k}^T \cdot \frac{\partial^2\langle\hat{S}\rangle_\alpha}{(\partial\vec{k})^2}|_{\vec{0}} \cdot \vec{k} + \dots \tag{25}$$

The right-hand side can be expressed as a sum of homogeneous polynomials $Q_\alpha^n(\vec{k})$ of consecutive order:

$$\langle\hat{S}\rangle_\alpha(\vec{k}) = \sum_{n\in\mathbf{N}} Q_\alpha^n(\vec{k}) \tag{26}$$

The momentum components k_i are $\mathcal{P}$-odd, while the spin texture components $\langle\hat{S}\rangle_\alpha(\vec{k})$, are $\mathcal{P}$-even. This implies $\langle\hat{S}\rangle(\vec{k}) = \langle\hat{S}\rangle(-\vec{k})$; $\langle\hat{S}\rangle$ is even in k_i. Because of this, the terms for odd n from the expression (26) can be discarded, leading to the following equation:

$$\langle\hat{S}\rangle_\alpha(\vec{k}) = \langle\hat{S}\rangle_\alpha(\vec{0}) + Q_\alpha^2(\vec{k}) + Q_\alpha^4(\vec{k}) \tag{27}$$

Homogeneous polynomials of order n are in bijection with symmetric tensors of the same order [37], so each Q_i^n can be expressed as a tensor $A_{\alpha j_1\dots j_n}$, where $Q_\alpha^n(\vec{k}) = A_{\alpha j_1\dots j_n} k_{j_1}\dots k_{j_n}$.
Since $\langle\hat{S}\rangle$ is a spin-vector, it transforms with the spin rotation matrices S as $\langle\hat{S}\rangle_\alpha \mapsto S_{\alpha\beta}\langle\hat{S}\rangle_\beta$. For the decomposition (27) to be compatible with this transformation law, Q_α^n at a set $\vec{k}$ must transform as the

components of a spin vector under a spin rotation S, that is $Q^n_\alpha \mapsto S_{\alpha\beta}Q^n_\beta$. Then, the three components Q^n_α can be expressed as a tensor of order $n+1$, with one spin and n spatial indices, symmetric in the spatial indices. Remarkably, the tensor $A_{\alpha ij}$ transforms as the tensor σ^α_{ij} for the $\mathcal{T}$-odd spin conductivity. Because of this, observation of non-transverse $\mathcal{T}$-odd (dissipative) spin conductivity may signify spin-splitting quadratic in k_i.
For $\vec{k}$ sufficiently close to $\vec{k_0}$, the expansion will be dominated by the lowest-order nonzero polynomials in δk_i.

2.4 Symmetry allowed tensors.

Each analysed tensor transforms in a specific way under spin rotations S and spatial isometries $\{R|\vec{v}\}$, determined by its indices. The indices of the tensor are determined by considering the law in which the tensor appears. For transport properties, such as conductivity σ_{ij} or the spin conductivity σ^α_{ij}, the tensors' parity under $\mathcal{T}$ inversion is determined by the Onsager reciprocity relations [33], or assumed. As an example, the Hall effect is described by

$$\vec{J} = \vec{\sigma}_H \times \vec{E} \tag{28}$$

where $\vec{J}$ is the current density, $\vec{E}$ is the electric field, and $\vec{\sigma}_H$ is the Hall vector. The current $\vec{J}$ transforms as a vector, and so does the electric field $\vec{E}$. To be compatible with these transformation laws, $\vec{\sigma}_H$ must be an axial vector. Furthermore, by the Onsager reciprocity relations it is $\mathcal{T}$-odd, so $\vec{\sigma}_H$ must transform as an $\mathcal{T}$-odd axial vector, i.e

$$\vec{\sigma}_H \mapsto \det(S)\det(R)R\cdot\vec{\sigma}_H \tag{29}$$

under the action of $\{S\|R|\vec{v}\}$.
By similar considerations, the magnetic moment $\vec{M}$ is a spin vector, which means that it is only affected by the spin rotations S, and under the action of $\{S\|R|\vec{v}\}$ it transforms as follows:

$$\vec{M} \mapsto S\cdot\vec{M} \tag{30}$$

The $\mathcal{T}$-odd spin conductivity tensor σ^α_{ij} has one spin index α and two spatial indices i,j, transforming under $\{S\|R|\vec{v}\}$ like:

$$\sigma^\alpha_{ij} \mapsto S^\alpha_\beta R^k_i R^l_j \sigma^\beta_{kl} \tag{31}$$

Lastly, the SHE conductivity tensor σ^α_i has one spin index α and one spatial axial vector under i, and transforms under $\{S\|R|\vec{v}\}$ as follows:

$$\sigma^\alpha_i \mapsto S^\alpha_\beta \det(R) R^j_i \sigma^\beta_j \tag{32}$$

Since all of the considered tensors correspond to macroscopic effects, they are unaffected by crystal translations by $\vec{v}$. To impose the symmetry constraints, only the spin or magnetic point groups need to be considered, which ignore translations.
The spaces of the analyzed tensors $(\vec{\sigma}_H, \sigma^\alpha_{ij}, \sigma^\alpha_i, \vec{M})$ are all constructed by forming a tensor product of the three basic modules V,A,M, corresponding to the three types of vectors under spin and spatial rotations, and in case of $\vec{\sigma}_H$, adding additional dependency on the $\mathcal{T}$-inversion. The *vector* module V is the vector space $\mathbb{R}^3$, whose elements $\vec{v} \in V$ are rotated by the spatial rotations. The axial vector module A is the vector space $\mathbb{R}^3$, whose elements $\vec{a} \in A$ behave as axial vectors under spatial rotations.

Finally, the spin module M is the vector space $\mathbb{R}^3$, whose elements $\vec{s} \in M$ rotate under spin rotations. The action of $\{S\|R\}$ on

Because the analyzed tensor spaces are tensor products of the three basic modules, they can be interpreted as $\mathbb{C}G$ modules under MPG or SPG, with corresponding representations formed by the tensor product. For example, a symmetry element $\{S\|R\}$ act on the space $M \otimes V^2$ of the spin conductivity tensor σ_{ij}^{α} as the matrix $S \otimes R \otimes R$, and this is how the group action is implemented in the calculations. The characters of the analyzed tensor modules are as follows:

$$\chi_H(S,R) = \det(S)\det(R)\mathrm{Tr}(R) \tag{33}$$
$$\chi_M(S,R) = \mathrm{Tr}(S) \tag{34}$$
$$\chi_{\sigma s}(S,R) = \mathrm{Tr}(S)\mathrm{Tr}(R)^2 \tag{35}$$
$$\chi_{sH}(S,R) = \det(R)\mathrm{Tr}(S)\mathrm{Tr}(R) \tag{36}$$

where $\{S\|R\}$ is written as a pair S,R for simplicity. The characters $\chi_H, \chi_M, \chi_s, \chi_{sH}$ correspond respectively to the Hall vector, the magnetic moment, the spin conductivity tensor, and the spin Hall effect tensor. If a tensor is allowed by symmetry, it must transform trivially under symmetry operations g[22]. By transforming trivially, it is meant that the tensor does not transform at all; it is fixed by all of the symmetry operations. For a tensor T this can be expressed as

$$gT = T \tag{37}$$

for every $g \in G$, with G being the symmetry group. This is because a symmetry of the magnetic crystal, be it in the spin group or magnetic group, leaves the crystal and its magnetic arrangement invariant, fixing all of its electromagnetic properties. By fixing all of the electromagnetic properties, the effects should also be fixed. There is another justification for this fact - if a tensor, which describes a property of the crystal (spin conductivity, spin splitting, anomalous Hall conductivity), were nonzero and would change under a symmetry of the magnetic crystal, the tensor would break this symmetry. The symmetries stem from the magnetic ordering, which is determined experimentally. Assuming the symmetries are unbroken, the symmetry group only allows for tensors that transform trivially under all of the symmetry operations.

The symmetry allowed tensors form a linear subspace T_{triv} of the tensor module T, as a linear combination of symmetry invariant tensors is also symmetry invariant. Since the symmetry operations act as identity on T_{triv}, T_{triv} is closed under the action of the symmetry group, and it is a submodule of T. This submodule is generated by some basis $T_1, \ldots, T_k$, the so-called allowed symmetry components. As T_i are symmetry invariant, the subspaces $\mathrm{Span}(T_i)$ are also submodules of T, furthermore

$$T_{triv} = \bigoplus_{i=1}^{k} \mathrm{Span}(T_i) \tag{38}$$

Each of the submodules spanned by T_i is isomorphic to the trivial submodule, a one-dimensional module equipped with the trivial representation, defined as

$$[g] = 1 \tag{39}$$

The trivial module is one-dimensional, so it is irreducible. The trivial module is associated with the trivial character, defined as $\chi_1(g) = 1$ for $g \in G$, where G is the symmetry group. This allows us to use representation theory to determine the dimension and basis of the trivial submodule T_{triv}. By

the orthogonality theorem (10), the dimension of T_{triv} is given by $\langle \chi_T, \chi_1 \rangle$, where χ_T is the character of the tensor module T. The basis $T_1, \ldots, T_k$ of T_{triv} can be obtained by using the equation (11) to construct the projection operator $1_{T_{triv}}$ from the representation $[\cdot]$ of G on the tensor T module, and calculating the eigenvectors of $1_{T_{triv}}$ associated with the eigenvalue $\lambda = 1$. The calculated T_i, the so-called allowed tensor components, form the basis of T_{triv}. All the symmetry allowed tensors T' can be uniquely expressed as a linear combination of the allowed components T_i, i.e.

$$T' = \lambda_1 T_1 + \cdots + \lambda_k T_k \tag{40}$$

where $\lambda_i \in \mathbb{R}$ are unique for T', which also includes the actual tensor describing an effect in the material, as long as the determined magnetic arrangement is accurate. All of the information from symmetry restrictions can be extracted by determining and interpreting the allowed tensor components T_i.

This method can be extended to any effect tensor, and a similar procedure is used in *MTENSOR* [38] and the newly developed *STENSOR* [22] programs on the BILBAO crystallographic server, which compute the allowed tensors for a given SPG or MPG. In this paper, the calculations are performed using basic representation theory and are extended to the study of spin textures, which, to the author's knowledge, has not been performed before in a similar way. The representation theory method is also used for the direct construction of tensors from lattice spins S_i and electron wavevectors $\vec{k}$.

2.4.1 Spin splitting near Γ point.

The method above is extended to the terms in the expansion of $\langle \hat{S} \rangle (\vec{k})$ near some $\vec{k}_0$, in this paper taken as $\vec{k}_0 = \vec{0}$, the Γ point. Each expansion term corresponds to a tensor of order $n+1$, with one spin and n spatial indices, symmetric in the spatial indices. By constructing the corresponding characters, the above method of enumeration of the symmetry-allowed components can be applied to these spin splitting tensors.

The tensor space of the spin splitting tensor of order $2m+1$ is constructed as a tensor product of a spin module M and $\mathcal{K}^{2m}$, the $2m$-th symmetric power of the wavevector module K. The spin module is defined as the space $\mathbb{R}^3$ transforming only under spin rotations, i.e under the action of a symmetry element $\{S||R|\vec{v}\}$, an element $\vec{m} \in M$ is mapped to $S \cdot \vec{m}$. Similarly, the wavevector module K is the space $\mathbb{R}^3$ transforming only under spatial rotations and time inversions. Under the action of $\{S||R|\vec{v}\}$, $\vec{k} \mapsto \det(S) R \cdot \vec{k}$. The $2m$-th tensor power K^{2m} of K consists of $2m$-th order tensors with all indices transforming as an element of K, while its subspace, the $2m$-th symmetric power $\mathcal{K}^{2m}$ of K, consists of the tensors in K^{2m} which are symmetric in all of the indices. By symmetric, it is meant that the tensors are invariant under any permutation of their indices. As only even symmetric powers of K are encountered in the expansion (27), the sign factor from the $\mathcal{T}$ inversion may be disregarded, and the action of $\{S||R|\vec{v}\}$ on K may be simplified to $\vec{k} \mapsto R \cdot \vec{k}$. This also allows for the treatment of the momentum indices of the full tensor as regular spatial indices, transforming only under spatial rotations.

The character of the spin module is given by $\chi_S = \mathrm{Tr}(S)$, but the character χ_{2m} of $\mathcal{K}^{2m}$ is more complicated. The characters of a symmetric power of any $\mathbb{C}G$ module V with an associated character χ can be expressed in terms of χ, and these expressions can be found in the literature. The following are the expressions for the characters of the second, fourth, and sixth symmetric powers of a module with character $\chi(R)$ [39]:

$$\chi_2(R) = \frac{1}{2}\left[\chi(R)^2 + \chi(R^2)\right] \tag{41}$$

$$\chi_4(R) = \frac{1}{24}\left[\chi(R)^4 + 8\chi(R)\chi(R^3) + 3\chi(R^2)^2 + 6\chi(R)^2\chi(R^2) + 6\chi(R^4)\right] \tag{42}$$

$$\begin{aligned}\chi_6(R) = \frac{1}{720}\Big[&\chi(R)^6 + 15\chi(R^2)\chi(R)^4 + 45\chi(R^2)^2\chi(R)^2 + 15\chi(R^2)^3 \\ &+ 40\chi(R^3)\chi(R)^3 + 120\chi(R^3)\chi(R^2)\chi(R) + 40\chi(R^3)^2 \\ &+ 90\chi(R^4)\chi(R)^2 + 90\chi(R^4)\chi(R^2) + 144\chi(R^5)\chi(R) + 120\chi(R^6)\Big].\end{aligned} \tag{43}$$

For symmetric powers of the K module, $\chi = \mathrm{Tr}(R)$. This leads to the following formula for the character of the spin splitting tensor:

$$\chi_{2m+1}(S,R) = \mathrm{Tr}(S)\chi_{2m}(R) \tag{44}$$

This character can be used to enumerate the spin splitting components allowed by SPG (no SOC) or MPG (SOC), which is done in this paper for quadratic, quartic, and sextic terms. Finding the components is more difficult, as it would necessitate a projection from the tensor space $S \otimes K^{2m}$ to the symmetric-in-spatial-indices subspace $S \otimes \mathcal{K}^{2m}$, and this is not done in this paper. An easier method is to find the symmetry-allowed elements of the $S \otimes K^{2m}$ space, and determine their symmetric part. For the quadratic terms, the spin splitting tensor transforms in the same way as the $\mathcal{T}$-odd spin conductivity tensor σ_{ij}^{α}, so the spin conductivity calculations can be repurposed to find the allowed quadratic spin splitting.

Additional restrictions on the spin splittings could be placed by verifying whether the allowed spin splitting components $\langle \hat{S} \rangle (\vec{k})$ or their combinations are allowed by the little group $G_{\vec{k}}$ at $\vec{k}$, but because of its complexity, this was not done in this paper.

3 Methods

3.1 The analyzed materials.

The materials analyzed are Mn_3Ir [40], Mn_3Sn [41], Mn_3Ge [34], Mn_3NiN [42], $MnTe_2$ [43], whose structures were downloaded as .mcif files from the MAGNDATA database. The magnetic order of these materials breaks neither translational nor inversion symmetry, and, except for $MnTe_2$, the materials exhibit high Néel temperatures, ranging from 262 to 960 K. These materials would not require cooling to cryogenic temperatures, making them promising candidates for spintronics devices. Various materials, which are not analysed in this study, have a magnetic arrangement equivalent to one of the studied materials, so the results of this study are applicable to these materials as well. For instance, the results for Mn_3Ir extend to Mn_3Pt, Mn_3GaN, and Mn_3ZnN. This is also true for the material Mn_3As, which has the same magnetic arrangement as Mn_3Sn or Mn_3Ge.

3.2 Determination of SSGs and MSGs.

Magnetic space groups (MSG) are determined using *spglib* library for Python [44], while spin space groups (SSG) are found with *spinspg* library [27], built on top of *spglib*. Mcif files are imported using *pymatgen* [45], and general calculations are performed with the help of *NumPy* [46]. The website *FINDSPINGROUP* [20] was used to screen suitable materials, look for SSG equivalence, and as a supplementary reference.
Spin point groups (SPG) and magnetic point groups (MPG) were determined by disregarding translations in the spin space group (SSG) or magnetic space group (MSG) elements. To unify the calculations, the elements of the MPG were expressed as a pair of matrices $\{S\|R\}$ instead of $\mathcal{T}^a R$. The spin rotation matrix S for the magnetic point group is given by $S = (-1)^a \det(R) R$.

3.3 Search for invariant tensor components.

The calculation By expressing the tensor products T of the base moduli V, A, M as a Kronecker product, the tensors in T can be flattened to vectors for computation. The representation of the symmetry group is formed by computing the corresponding Kronecker products of the base representations $R, \det(R), S$ of the symmetry elements $\{S\|R\}$. The constructed representation is used to find the projection operator 1_{triv} using the equation (11). For the elements $\vec{u}$ in the invariant subspace U, $T\vec{u} = \vec{u}$, while for $\vec{v} \in V - U$, $T\vec{v} = \vec{0}$. By selecting the eigenvectors $\vec{w}$ of T associated with an eigenvalue of 1, the basis of the invariant module is found. In this project, the eigenvalue problems were solved using the SciPy package [47], while the rest of the calculations were handled with *Numpy* [46].
The number of independent tensor components allowed by the symmetry was calculated by forming the inner product $\langle \chi_T, \chi_1 \rangle$ of the trivial character χ_1 with the character of the tensor module χ_T. This was calculated for all of the effect tensors, and the tensors describing quadratic, quartic, and sextic terms in k_i allowed in the expansion of $\langle \hat{S} \rangle (\vec{k})$ near the Γ point. This character product should be equal to the number of independent allowed tensor components, and for the effect tensors it was used to verify the previous calculations. An additional method of validation was used, in which the symmetry elements were applied to the allowed tensor components, to check if they are invariant under the group action.

4 Results

4.1 Symmetry constraints on the effect tensors.

The third-order tensors σ_{ij}^{α} in this section are written as three matrices $\sigma_{ij}^{1}, \sigma_{ij}^{2}, \sigma_{ij}^{3}$ separated by vertical bars. The second order $\mathcal{T}$-odd SHE tensors σ_{i}^{α} are written as three vectors $\sigma_{i}^{1}, \sigma_{i}^{2}, \sigma_{i}^{3}$ separated by vertical bars as well. All indices, except the spatial indices of σ_{ij}^{α} for Mn_3NiN, are always presented in a Cartesian basis, with y axis coinciding with the crystal $\vec{b}$ direction, and z axis coinciding with the crystal $\vec{c}$ direction. For cubic Mn_3Ir, $MnTe_2$, the crystal basis coincides with the Cartesian basis. This is not true for the remaining materials, which are all hexagonal.

4.1.1 Mn_3Ir

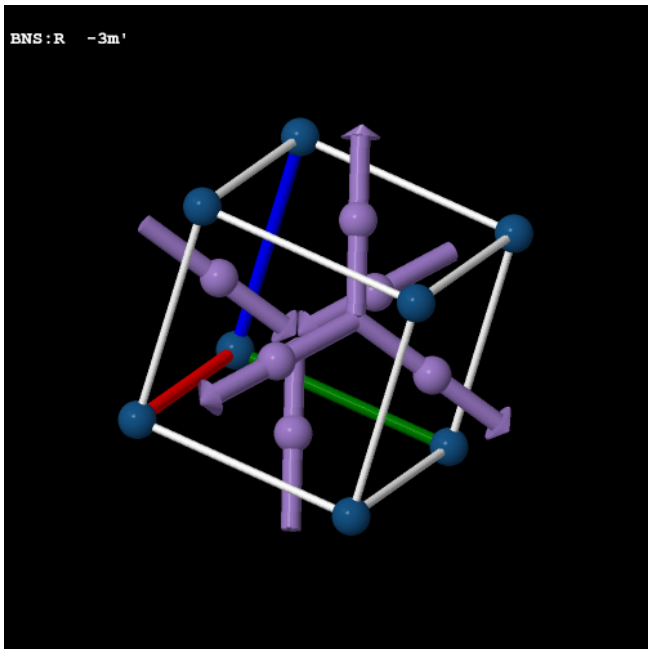

Figure 3: Magnetic ordering of Mn_3Ir [40].

Without SOC, the symmetries of the material permit only one out of 27 components of the spin conductivity tensor. The component is proportional to the tensor below, with the three matrices being conductivity tensors for the three spin polarizations, which is diagonal.

$$\left(\begin{array}{ccc|ccc|ccc} 2 & 0 & 0 & -1 & 0 & 0 & -1 & 0 & 0 \\ 0 & -1 & 0 & 0 & 2 & 0 & 0 & -1 & 0 \\ 0 & 0 & -1 & 0 & 0 & -1 & 0 & 0 & 2 \end{array}\right)$$

As this tensor is symmetric in the spatial indices, it corresponds to the SOC-independent quadratic term of spin-splitting near the Γ point, given by

$$\left(2k_x^2 - k_y^2 - k_z^2,\ -k_x^2 + 2k_y^2 - k_z^2,\ -k_x^2 - k_y^2 + 2k_z^2\right).$$

The presence of SOC permits the existence of a magnetic moment oriented along [111], and a Hall vector oriented in the same direction. It also allows for four additional components of the $\sigma_{ij}^{s\alpha}$ tensor,

increasing the number to five in total. One component antisymmetric in the spatial indices is allowed, which may be written as a matrix.

$$\left(\begin{array}{c|c|c} 0 & 1 & -1 \\ -1 & 0 & 1 \\ 1 & -1 & 0 \end{array}\right)$$

Remarkably, this matrix is antisymmetric as well, and the allowed tensor component σ_{ij}^{α} is proportional to the Levi-Civita symbol $\varepsilon_{ij}^{\alpha}$.

4.1.2 Mn_3Ge

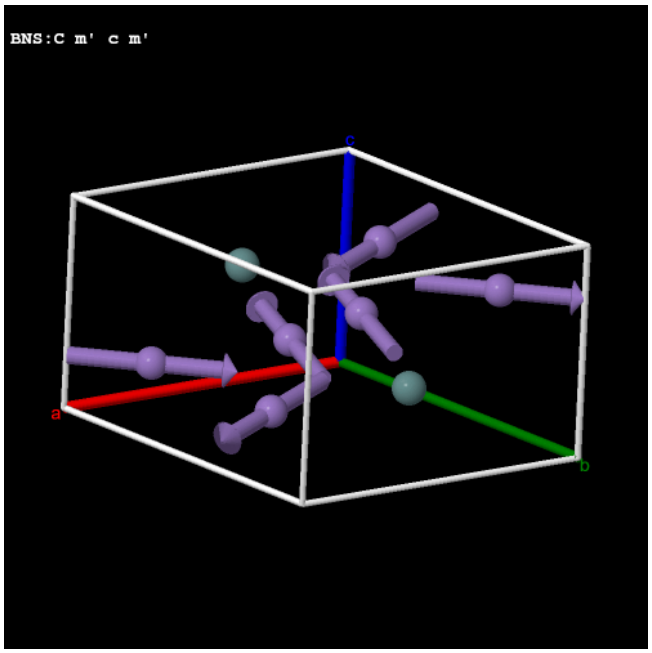

Figure 4: Magnetic ordering of Mn_3Ge [34]

Free of SOC, the material allows for one component of spin conductivity, proportional to the following tensor, whose spatial indices are in the crystal basis.

$$\left(\begin{array}{ccc|ccc|ccc} 0 & -11.196 & 0 & 14.928 & -1 & 0 & 0 & 0 & 0 \\ -11.196 & 1.5 & 0 & -1 & -8.33 & 0 & 0 & 0 & 0 \\ 0 & 0 & 0 & 0 & 0 & 0 & 0 & 0 & 0 \end{array}\right)$$

This tensor is symmetric in spatial indices, so it corresponds to a quadratic term of spin-splitting near the Γ point. This splitting is given by:

$$\left(-\sqrt{3}k_2^2 - 2\sqrt{3}k_1k_2,\ 2k_1^2 + 2k_1k_2 - k_2^2,\ 0\right)$$

where k_i are the coordinates of the wavevector given in the crystal basis.
Lifting of SO leads to a possible in-plane magnetic moment and Hall vector in the $(1\bar{1}00)$ direction. It also leads to seven allowed spin conductivity components. Four of them lead to the generation of

in-plane, in-plane polarized current by in-plane electric fields, two for z-polarized current in the z-direction caused by an electric field oriented along the z-direction, and one corresponds to an in-plane electric field generating an in-plane polarized spin current in the z-direction. The spin conductivity components can be combined to form two independent transverse components, which can be written as the following matrices.

$$\left(\begin{array}{c|c|c} 0 & 0 & 1+\sqrt{3} \\ 0 & 0 & 1 \\ 0 & 0 & 0 \end{array}\right) \left(\begin{array}{c|c|c} 0 & 0 & 0 \\ 0 & 0 & 0 \\ 1+\sqrt{3} & 1 & 0 \end{array}\right)$$

None of the invariant tensors allows for the generation of in-plane spin current by E_z, and every in-plane spin current is polarized in-plane.

4.1.3 Mn_3Sn

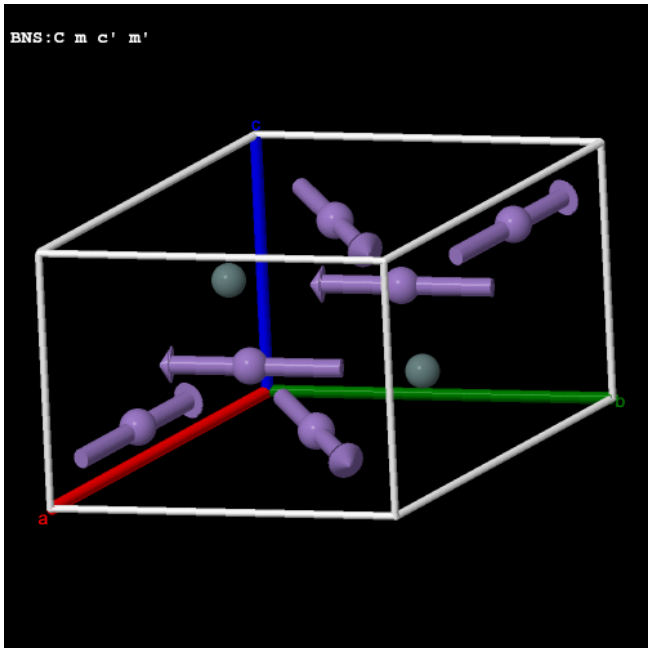

Figure 5: Magnetic ordering of Mn_3Sn [41].

Without SOC, this material allows for one component of the spin conductivity tensor, proportional to the tensor below.

$$\left(\begin{array}{ccc|ccc|ccc} -1.366 & -1.683 & 0 & 2.366 & -1.183 & 0 & 0 & 0 & 0 \\ -1.683 & 1 & 0 & -1.183 & -1.183 & 0 & 0 & 0 & 0 \\ 0 & 0 & 0 & 0 & 0 & 0 & 0 & 0 & 0 \end{array}\right)$$

This tensor is symmetric in spatial indices, so it corresponds to a quadratic term of spin-splitting near the Γ point. This splitting is given by:

$$\left(k_1^2 + 4k_1k_2 + k_2^2,\ -\sqrt{3}k_1^2 + \sqrt{3}k_2^2,\ 0\right)$$

where k_i are the coordinates of the wavevector given in the crystal basis.
SOC allows for in-plane magnetic moment and Hall vector in $[01\bar{1}0]$ direction, and seven spin conductivity components, allowing two independent transverse components, written as matrices below. The row number corresponds to the spin polarization index, while the column number is the spatial axial index.

$$\left(\begin{array}{c|c|c} 0 & 0 & 0 \\ 0 & 0 & 0 \\ 14.928 & -1 & 0 \end{array}\right) \left(\begin{array}{c|c|c} 0 & 0 & 14.928 \\ 0 & 0 & 1 \\ 0 & 0 & 0 \end{array}\right)$$

The invariant spin conductivity tensor components restrict the spin currents generated by E_z to the $(10\bar{1}0)$ plane, while the electric field in the $[10\bar{1}0]$ direction can only generate a current in the (0001) plane.

4.1.4 Mn_3NiN

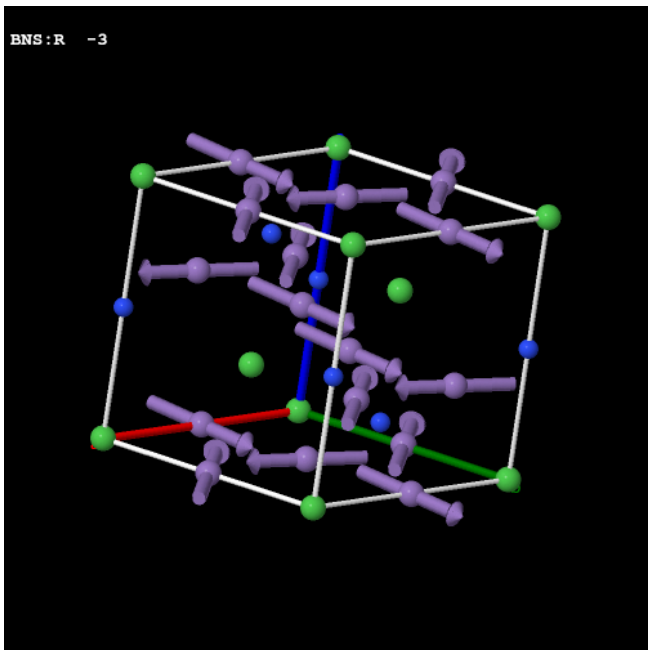

Figure 6: Magnetic ordering of Mn_3NiN [42].

In the absence of SOC, the material allows one spin conductivity component, presented below with the spatial coordinates in the crystal basis, for clarity.

$$\left(\begin{array}{ccc|ccc|ccc} 0.577 & 0 & 0 & -0.018 & 0 & 0 & -0.025 & 0 & 0 \\ 0 & -0.315 & 0 & 0 & -0.279 & 0 & 0 & -0.395 & 0 \\ 0 & 0 & -0.261 & 0 & 0 & 0.297 & 0 & 0 & 0.420 \end{array}\right)$$

The matrices σ_{ij}^{α} are diagonal, similarly to the spin conductivity component allowed by the SPG of Mn_3Ir. When viewed in the Cartesian basis, this tensor is symmetric in spatial indices, so it

corresponds to a quadratic term of spin-splitting near the Γ point. This splitting is proportional to the following expression:

$$\left(0.577\,k_1^2 - 0.315\,k_2^2 - 0.261\,k_3^2,\ -0.018\,k_1^2 - 0.279\,k_2^2 + 0.297\,k_3^2,\ -0.025\,k_1^2 - 0.395\,k_2^2 + 0.420\,k_3^2\right)$$

where k_i are the coordinates of the wavevector given in the crystal basis.
With SOC, a magnetization in the $[\bar{1}101]$ direction is possible. A Hall vector in the same direction is also allowed by symmetry. Nine independent components of the spin conductivity are allowed, with three antisymmetric in the spatial coordinates. None of the components is sparse or easily interpretable.

4.1.5 $MnTe_2$

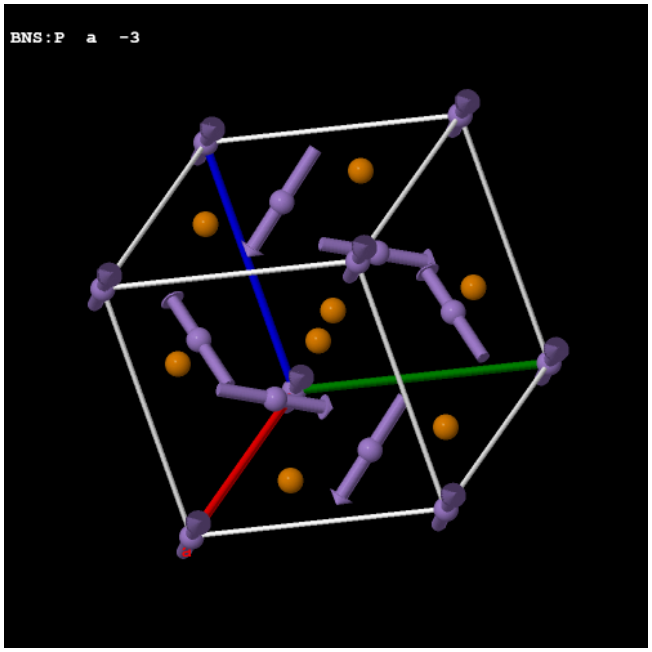

Figure 7: Magnetic ordering of $MnTe_2$ [43].

Without SOC, this material allows for two spin conductivity components, one antisymmetric and one symmetric in the spatial indices. The antisymmetric component can be written as

$$\left(\begin{array}{c|c|c} -1 & 0 & 0 \\ 0 & -1 & 0 \\ 0 & 0 & -1 \end{array}\right)$$

The symmetric component is proportional to the following tensor, with spatial indices in the crystal basis.

$$\left(\begin{array}{ccc|ccc|ccc} 0 & 0 & 0 & 0 & 0 & 1 & 0 & 1 & 0 \\ 0 & 0 & 1 & 0 & 0 & 0 & 1 & 0 & 0 \\ 0 & 1 & 0 & 1 & 0 & 0 & 0 & 0 & 0 \end{array}\right)$$

This symmetric tensor corresponds to the SOC-independent quadratic term of spin-splitting near the Γ point, proportional to

$$\left(k_y k_z,\ k_x k_z,\ k_x k_y\right)$$

Curiously, the spin space group of $MnTe_2$ is equal to its magnetic space group, so the presence of SOC does not allow for any additional invariant tensor components. The presence of SOC does not allow for a magnetic moment, nor the anomalous Hall effect, which would require further breaking of the magnetic symmetry.

4.2 Expansion of $\langle \hat{S} \rangle (\vec{k})$ in the powers of k_i near the Γ point.

	No SOC			SOC		
	Quadratic	Quartic	Sextic	Quadratic	Quartic	Sextic
Mn_3Ir	1	2	3	4	9	16
Mn_3Ge	1	3	5	5	12	22
Mn_3Sn	1	3	5	5	12	22
Mn_3NiN	1	2	3	6	15	28
$MnTe_2$	1	3	6	1	3	6

Table 1: Number of the allowed spin splitting components with and without SOC for the analyzed materials.

The number of terms in the expansion of $\langle \hat{S} \rangle (\vec{k})$ near $\vec{k} = \vec{0}$ of second, fourth, and sixth order in k_i was calculated by forming the inner product of the tensor characters χ_T with the trivial character χ_1. As the tensors describing second-order spin splitting transform in the same manner as the spin conductivity tensor σ_{ij}^{α}, the allowed σ_{ij}^{α} components correspond to the allowed second-order splitting terms. If $(A|B|C)$ is an allowed component of σ_{ij}^{α}, where A, B, C are 3×3 matrices corresponding to $\sigma_{ij}^{1}, \sigma_{ij}^{2}, \sigma_{ij}^{3}$, then

$$\left(\vec{k}^T \cdot A \cdot \vec{k},\ \vec{k}^T \cdot B \cdot \vec{k},\ \vec{k}^T \cdot C \cdot \vec{k}\right)$$

is an allowed quadratic spin-splitting term. Such a calculation was performed for the SOC case in all of the analyzed materials.
Spin-splitting terms of the order zero transform as a spin vector, identically to the magnetic moment vector $\vec{M}$, and the results for the weak ferromagnetic moment directly correspond to zeroth order (constant) spin-splitting.

5 Discussion

Each of the analyzed materials has components of the $\mathcal{T}$-odd spin conductivity tensor σ_{ij}^{α} allowed by the spin point group, allowing for the conversion of electric current into spin current. Without SOC, the number of allowed spin conductivity components is low, which might explain the high anisotropy observed in the spin Hall effect observed in some of the materials [48]. Additionally, all of the materials allow for exactly one quadratic spin-splitting term, which does not require SOC. Without SOC, the materials can also have quartic and sextic terms in the expansion of $\langle \hat{S} \rangle (\vec{k})$ near $\vec{k} = \vec{0}$, with higher order spin-splitting having more allowed independent components. For some of the materials, such as Mn_3Ge, Mn_3Sn, or $MnTe_2$, geometric constraints on the spin current could be made even with spin-orbit coupling - as an example, in Mn_3Ge E_z only generates a spin current in the z-direction, always polarized in the plane $[0001]$.

Unsurprisingly, none of the materials exhibit the anomalous Hall effect in the absence of SOC. In the absence of SOC, the topological Hall effect can arise in certain non-coplanar arrangements. The only non-coplanar antiferromagnet considered in this paper was $MnTe_2$, which does not allow AHE even with SOC. All the other materials studied in this paper can exhibit AHE and a weak ferromagnetic moment with SOC. Under magnetic point groups, the magnetic moment and the Hall vector both transform as an $\mathcal{T}$-odd axial vector, as well as the $\vec{g}(\omega)$ vector corresponding to the magneto-optic Kerr effect [31]. The results of the representation theory calculations depend only on how the tensors transform under group elements, so the results for AHE are directly extensible to the magneto-optic Kerr effect. Then Mn_3Ge, Mn_3Ir, Mn_3NiN, Mn_3Sn, and by extension all of the materials with magnetic arrangements equivalent to these four, can exhibit the Kerr effect, while $MnTe_2$ cannot.

6 Conclusion

With the use of basic representation theory, it was demonstrated that all of the analyzed materials allow for SOC-free $\mathcal{T}$-odd spin conductivity, and quadratic spin-splitting terms in the expansion of $\langle\hat{S}\rangle(\vec{k})$ near the Γ point. With SOC, all of the materials permit $\mathcal{T}$-odd spin Hall effect. The magnetic point groups of the materials, except $MnTe_2$, allow for weak ferromagnetism and a Hall vector in a specific direction in the magnetic cell. The independent tensor components of $\mathcal{T}$-odd spin conductivity σ_{ij}^{α} and $\mathcal{T}$-odd spin Hall effect σ_{i}^{α}, which form the basis for the space of the symmetry allowed tensors, were determined for the magnetic point group and spin point group of the studied materials, and the results agree with the literature [19]. The number of symmetry-allowed components of the spin conductivity independent of SOC is low, which might explain the high anisotropy of spin current generation observed in Mn_3Pt [48], which shares the same magnetic arrangement with Mn_3Ir. Furthermore, by interpreting the allowed spin conductivity components, restrictions can be placed on the effect. For example, in Mn_3Ge E_z only generates a spin current in the z-direction, always polarized in the plane $[0001]$. In general, the findings of this paper agree with experiments [8] [9] [15] [16] [48] [49].

One important result of this paper is the linking of spin-splitting terms quadratic in k_i with the $\mathcal{T}$-odd spin Hall conductivity. This result suggests that the presence $\mathcal{T}$-odd spin Hall conductivity is always accompanied by quadratic spin splitting, analogously to how the anomalous Hall effect is accompanied by some magnetic moment, which is associated with constant spin-splitting.

Overall, the goal of the study was fulfilled. Representation theory arguments were successfully used to analyze various effects, such as AHE, $\mathcal{T}$-odd SHE, or spin-splitting. The results agree with the experiments, and the analyzed materials are promising platforms for spintronics applications. The analysis performed in this paper can be extended in various directions, by studying more non-collinear antiferromagnets, or by considering other effects. The allowed components of higher-order spin-splitting can be explicitly evaluated by constructing a projection operator from the tensor space $M \otimes \mathcal{K}^{2m}$ onto its trivial submodule. One possible method of doing that may be by composing the projection operator 1_{symm}, projecting $M \otimes K^{2m}$ onto its symmetric submodule $M \otimes \mathcal{K}^{2m}$ with the projection operator 1_{triv}, projecting $M \otimes K^{2m}$ onto its trivial submodule. The composition $1_{triv}1_{symm}$ is a projection, which is nonzero only for the elements in the trivial submodule of $M \otimes \mathcal{K}^{2m}$. The formalism can also be used to determine the components of $\langle\hat{S}\rangle(\vec{k})$ allowed by the little group at $\vec{k}$, which could be used to place additional restrictions on the symmetry-allowed expansion (27) near the Γ point. For instance, some expansion terms allowed by SPG or MPG might be incompatible with these additional constraints and could only arise in combination with another allowed expansion term, further limiting the number of allowed expansion components. Finally, the method could be extended to collinear antiferromagnets, which would require adapting the approach for their infinite spin groups. The spin-only group for a collinear arrangement is isomorphic to $SO(2) \rtimes \{E, Z_2\}$, including all rotations around the spin axis and all reflections across planes containing the spin axis. These operations force spin vectors to be oriented along the spin axis. By manually placing such a restriction, the spin-only group can be reduced to $\{E, Z_2\}$, i.e, the identity E and the reflection Z_2 across a plane containing the spin axis. This restriction would make the spin point group finite, making it possible to use the representation theory formalism presented in this paper.

Bibliography

[1] A. Métioui, "Brief historical review about magnetism: From the ancient greeks up to the beginning of the 20th century," *Journal of Biomedical Research & Environmental Sciences*, vol. 3, pp. 1101–1107, September 2022. Published 23 September 2022; received 20 August 2022, accepted 19 September 2022.

[2] N. F. Kharchenko, "On seven decades of antiferromagnetism," *Low Temperature Physics*, vol. 31, pp. 633–634, August–September 2005.

[3] P. J. Rajput, S. U. Bhandari, and G. Wadhwa, "A review on—spintronics an emerging technology," *Silicon*, vol. 14, pp. 9195–9210, October 2022.

[4] S. Bhatti, A. Fabrizio, E. Allahyarov, *et al.*, "Spintronics based random access memory: A review," *Materials Today*, vol. 20, pp. 530–548, November 2017.

[5] B. H. Rimmler, B. Pal, and S. S. P. Parkin, "Non-collinear antiferromagnetic spintronics," *Nature Reviews Materials*, vol. 10, pp. 109–127, February 2025. Accepted 2 July 2024; Published 29 August 2024.

[6] D. Xiong, Y. Jiang, K. Shi, A. Du, Y. Yao, Z. Guo, D. Zhu, K. Cao, S. Peng, W. Cai, D. Zhu, and W. Zhao, "Antiferromagnetic spintronics: An overview and outlook," *Fundamental Research*, vol. 2, pp. 522–534, April 2022.

[7] H. Chen, Q. Niu, and A. H. MacDonald, "Anomalous hall effect arising from noncollinear antiferromagnetism," *Phys. Rev. Lett.*, vol. 112, p. 017205, January 2014. Received 3 October 2013; Published 10 January 2014.

[8] S. Nakatsuji, N. Kiyohara, and T. Higo, "Large anomalous hall effect in a noncollinear antiferromagnet at room temperature," *Nature*, vol. 527, pp. 212–215, 2015.

[9] A. K. Nayak, J. E. Fischer, Y. Sun, B. Yan, J. Karel, A. C. Komarek, C. Shekhar, N. Kumar, W. Schnelle, J. Kübler, C. Felser, and S. S. P. Parkin, "Large anomalous hall effect driven by non-vanishing berry curvature in the non-collinear antiferromagnet Mn_3Ge," *Science Advances*, vol. 2, no. 4, p. e1501870, 2016.

[10] L. Šmejkal, R. González-Hernández, T. Jungwirth, and J. Sinova, "Crystal time-reversal symmetry breaking and spontaneous hall effect in collinear antiferromagnets," *Science Advances*, vol. 6, p. eaaz8809, June 2020.

[11] L. Šmejkal, A. H. MacDonald, J. Sinova, S. Nakatsuji, and T. Jungwirth, "Anomalous hall antiferromagnets," *Nature Reviews Materials*, vol. 7, pp. 482–496, 2022.

[12] M. K. Ray, M. Fu, Y. Chen, T. Chen, T. Nomoto, S. Sakai, M. Kitatani, M. Hirayama, S. Imajo, T. Tomita, A. Sakai, D. Nishio-Hamane, G. T. McCandless, M.-T. Suzuki, Z. Xu, Y. Zhao, T. Fennell, Y. Kohama, J. Y. Chan, R. Arita, C. Broholm, and S. Nakatsuji, "Zero-field hall effect emerging from a non-fermi liquid in a collinear antiferromagnet $V_{1/3}NbS_2$," *Nature Communications*, vol. 16, 2025.

[13] L. Šmejkal, J. Sinova, and T. Jungwirth, "Beyond conventional ferromagnetism and antiferromagnetism: A phase with nonrelativistic spin and crystal rotation symmetry," *Physical Review X*, vol. 12, p. 031042, September 2022.

[14] L. Šmejkal, J. Sinova, and T. Jungwirth, "Emerging research landscape of altermagnetism," *Physical Review X*, vol. 12, p. 040501, December 2022.

[15] G. Gurung, M. Elekhtiar, Q.-Q. Luo, D.-F. Shao, and E. Y. Tsymbal, "Nearly perfect spin polarization of noncollinear antiferromagnets," *Nature Communications*, vol. 15, November 2024. Received: 18 May 2024; Accepted: 13 November 2024; Published: 26 November 2024.

[16] Y.-P. Zhu, X. Chen, X.-R. Liu, Y. Liu, P. Liu, H. Zha, G. Qu, C. Hong, J. Li, Z. Jiang, X.-M. Ma, Y.-J. Hao, M.-Y. Zhu, W. Liu, M. Zeng, S. Jayaram, M. Lenger, J. Ding, S. Mo, K. Tanaka, M. Arita, Z. Liu, M. Ye, D. Shen, J. Wrachtrup, Y. Huang, R.-H. He, S. Qiao, Q. Liu, and C. Liu, "Observation of plaid-like spin splitting in a noncoplanar antiferromagnet," *Nature*, vol. 626, pp. 523–528, February 2024. Published online: 14 February 2024.

[17] A. D. Din, O. J. Amin, P. Wadley, and K. W. Edmonds, "Antiferromagnetic spintronics and beyond," *npj Spintronics*, vol. 2, p. 25, 2024. Review article.

[18] L.-D. Yuan, Z. Wang, J.-W. Luo, and A. Zunger, "Strong influence of nonmagnetic ligands on the momentum-dependent spin splitting in antiferromagnets," *Physical Review B*, vol. 103, no. 22, p. 224410, 2021.

[19] J. Železný, Y. Zhang, C. Felser, and B. Yan, "Spin-polarized current in noncollinear antiferromagnets," *Physical Review Letters*, vol. 119, p. 187204, November 2017.

[20] X. Chen, J. Ren, Y. Zhu, Y. Yu, A. Zhang, P. Liu, J. Li, Y. Liu, C. Li, and Q. Liu, "Enumeration and representation theory of spin space groups," *Physical Review X*, vol. 14, p. 031038, August 2024.

[21] P. Liu, J. Li, J. Han, X. Wan, and Q. Liu, "Spin-group symmetry in magnetic materials with negligible spin-orbit coupling," *Physical Review X*, vol. 12, no. 2, p. 021016, 2022.

[22] J. Etxebarria, J. M. Perez-Mato, E. S. Tasci, and L. Elcoro, "Crystal tensor properties of magnetic materials with and without spin–orbit coupling. application of spin point groups as approximate symmetries," *Acta Crystallographica Section A: Foundations and Advances*, vol. 81, pp. 1–22, 2025.

[23] W. F. Brinkman and R. J. Elliott, "Theory of spin-space groups," *Proceedings of the Royal Society of London. Series A, Mathematical and Physical Sciences*, vol. 294, no. 1437, pp. 343–358, 1966.

[24] D. B. Litvin and W. Opechowski, "Spin groups," *Physica*, vol. 76, no. 3, pp. 538–554, 1974.

[25] Z. Xiao, J. Zhao, Y. Li, R. Shindou, and Z.-D. Song, "Spin space groups: Full classification and applications," *Physical Review X*, vol. 14, p. 031037, August 2024.

[26] Y. Jiang, Z. Song, T. Zhu, Z. Fang, H. Weng, Z.-X. Liu, J. Yang, and C. Fang, "Enumeration of spin-space groups: Toward a complete description of symmetries of magnetic orders," *Physical Review X*, vol. 14, p. 031039, August 2024.

[27] K. Shinohara, A. Togo, H. Watanabe, T. Nomoto, I. Tanaka, and R. Arita, "Algorithm for spin symmetry operation search," *Acta Crystallographica Section A: Foundations and Advances*, vol. 80, pp. 94–103, January 2024.

[28] G. James and M. Liebeck, *Representations and Characters of Groups*. Cambridge: Cambridge University Press, 2nd ed., 2001.

[29] M. Mostovoy, "Landau theory," 2024. Lecture notes for Many-Particles Physics 2, Zernike Institute for Advanced Materials, University of Groningen.

[30] D. Boldrin, I. Samathrakis, J. Zemen, A. Mihai, B. Zou, F. Johnson, B. D. Esser, D. W. McComb, P. K. Petrov, H. Zhang, and L. F. Cohen, "Anomalous hall effect in noncollinear antiferromagnetic mn_3nin thin films," *Phys. Rev. Materials*, vol. 3, p. 094409, September 2019. Received 22August2019; Published 23September2019.

[31] M. Mostovoy, "Phenomenology of altermagnets," *arXiv preprint*, 2025. Version 1, June 3, 2025.

[32] C. Kittel, *Introduction to Solid State Physics*. Hoboken, NJ: John Wiley & Sons, 8th ed., 2005.

[33] N. Nagaosa, J. Sinova, S. Onoda, A. H. MacDonald, and N. P. Ong, "Anomalous hall effect," *Reviews of Modern Physics*, vol. 82, no. 2, pp. 1539–1592, 2010.

[34] J.-R. Soh, F. de Juan, N. Qureshi, H. Jacobsen, H.-Y. Wang, Y.-F. Guo, and A. T. Boothroyd, "Ground-state magnetic structure of mn_3ge," *Physical Review B*, vol. 101, p. 140411(R), April 2020.

[35] I. V. Solovyev, S. A. Nikolaev, and A. Tanaka, "Altermagnetism and weak ferromagnetism," *arXiv preprint*, 2025. arXiv:2503.23735 [cond-mat.mtrl-sci], submitted April 1, 2025.

[36] J. Sinova, S. O. Valenzuela, J. Wunderlich, C. H. Back, and T. Jungwirth, "Spin hall effects," *Reviews of Modern Physics*, vol. 87, no. 4, pp. 1213–1260, 2015.

[37] P. Comon, G. Golub, L.-H. Lim, and B. Mourrain, "Symmetric tensors and symmetric tensor rank," *SIAM Journal on Matrix Analysis and Applications*, vol. 30, no. 3, pp. 1254–1279, 2008.

[38] S. V. Gallego, J. Etxebarria, L. Elcoro, E. S. Tasci, and J. M. Perez-Mato, "Automatic calculation of symmetry-adapted tensors in magnetic and non-magnetic materials: a new tool of the bilbao crystallographic server," *Acta Crystallographica Section A: Foundations and Advances*, vol. 75, pp. 438–447, April 2019.

[39] X.-F. Zhou and P. Pulay, "Characters for symmetric and antisymmetric higher powers of representations: Application to the number of anharmonic force constants in symmetrical molecules," *Journal of Computational Chemistry*, vol. 10, no. 7, pp. 935–938, 1989.

[40] I. Tomeno, H. N. Fuke, H. Iwasaki, M. Sahashi, and Y. Tsunoda, "Magnetic neutron scattering study of ordered mn_3ir," *Journal of Applied Physics*, vol. 86, no. 7, pp. 3853–3856, 1999.

[41] P. J. Brown, V. Núñez, F. Tasset, J. B. Forsyth, and P. Radhakrishna, "Determination of the magnetic structure of mn_3sn using generalized neutron polarization analysis," *Journal of Physics: Condensed Matter*, vol. 2, no. 47, pp. 9409–9422, 1990.

[42] M. Wu, C. Wang, Y. Sun, L. Chu, J. Yan, D. Chen, Q. Huang, and J. W. Lynn, "Magnetic structure and lattice contraction in mn_3nin," *Journal of Applied Physics*, vol. 114, no. 12, p. 123902, 2013.

[43] P. Burlet, E. Ressouche, B. Malaman, R. Welter, J. Sanchez, and P. Vulliet, "Noncollinear magnetic structure of $mnte_2$," *Phys. Rev. B*, vol. 56, pp. 14013–14019, December 1997.

[44] A. Togo and I. Tanaka, "Spglib: a software library for crystal symmetry search," *arXiv preprint*, 2018.

[45] S. P. Ong, W. D. Richards, A. Jain, G. Hautier, M. Kocher, S. Cholia, D. Gunter, V. Chevrier, K. A. Persson, and G. Ceder, "Python materials genomics (pymatgen): A robust, open-source python library for materials analysis," *Computational Materials Science*, vol. 68, pp. 314–319, 2013.

[46] C. R. Harris, K. J. Millman, S. J. van der Walt, R. Gommers, P. Virtanen, D. Cournapeau, E. Wieser, J. Taylor, S. Berg, N. J. Smith, R. Kern, M. Picus, S. Hoyer, M. H. van Kerkwijk, M. Brett, A. Haldane, J. F. del Río, M. Wiebe, P. Peterson, P. Gérard-Marchant, K. Sheppard, T. Reddy, W. Weckesser, H. Abbasi, C. Gohlke, and T. E. Oliphant, "Array programming with NumPy," *Nature*, vol. 585, pp. 357–362, 2020.

[47] P. Virtanen, R. Gommers, T. E. Oliphant, M. Haberland, T. Reddy, D. Cournapeau, E. Burovski, P. Peterson, W. Weckesser, J. Bright, S. J. van der Walt, M. Brett, J. Wilson, K. J. Millman, N. Mayorov, A. R. J. Nelson, E. Jones, R. Kern, E. Larson, C. J. Carey, İ. Polat, Y. Feng, E. W. Moore, J. VanderPlas, D. Laxalde, J. Perktold, R. Cimrman, I. Henriksen, E. A. Quintero, C. R. Harris, A. M. Archibald, A. H. Ribeiro, F. Pedregosa, P. van Mulbregt, and S. . Contributors, "Scipy 1.0: fundamental algorithms for scientific computing in python," *Nature Methods*, vol. 17, pp. 261–272, 2020.

[48] C. Cao, S. Chen, R.-C. Xiao, Z. Zhu, G. Yu, Y. Wang, X. Qiu, L. Liu, T. Zhao, D.-F. Shao, Y. Xu, J. Chen, and Q. Zhan, "Anomalous spin current anisotropy in a noncollinear antiferromagnet," *Nature Communications*, vol. 14, 2023.

[49] S. Hu, D.-F. Shao, H. Yang, C. Pan, Z. Fu, M. Tang, Y. Yang, W. Fan, S. Zhou, E. Y. Tsymbal, and X. Qiu, "Efficient perpendicular magnetization switching by a magnetic spin hall effect in a noncollinear antiferromagnet," *Nature Communications*, vol. 13, p. 4447, 2022.

Acknowledgments

First of all, I would like to thank prof. Dr. Maxim Mostovoy and prof. Dr. Holger Waalkens for being my examiner and assisting me throughout the project. This project would not be possible without the Bilbao Crystallographic server, especially the MAGNDATA database, and the website FINDSPINGROUP. The Python library *sinspg* was essential to determine the spin groups of the materials, and the calculation would not be possible without the specialized *spglib* and *pymatgen* libraries. Perplexity AI and Google Scholar were essential in the literature search. Finally, I would like to thank my girlfriend, Kinga, for proofreading and generally supporting me.

Appendices

A Symmetry allowed tensor components

A.1 Mn_3Ir

Spin conductivity components allowed by the magnetic point group for Mn_3Ir. The matrices separated by vertical lines represent the components of the spin conductivity σ_{ij}^{α} for spin polarization in a Cartesian basis. Because Mn_3Ir is cubic, the Cartesian basis can be oriented so that the x, y, z axes coincide with the crystal directions $[100], [010], [001]$. The basis in which the tensor is presented is rotated compared to this basis, by a rotation around the direction perpendicular to the plane spanned by $[111]$ and $[001]$, such that the position $[111]$ is rotated to the z-axis. In this rotated basis, the z axis is in the direction of the allowed weak ferromagnetic moment, and all five tensors assume a similar form.

$$\left(\begin{array}{ccc|ccc|ccc} 1 & -1 & 2 & -1 & -1 & 0 & 2 & 0 & 0 \\ -1 & -1 & 0 & -1 & 1 & 2 & 0 & 2 & 0 \\ 2 & 0 & 0 & 0 & 2 & 0 & 0 & 0 & 2 \end{array}\right)$$

$$\left(\begin{array}{ccc|ccc|ccc} 1 & -1 & -7.433 & -1 & -1 & 0 & 2 & 0 & 0 \\ -1 & -1 & 0 & -1 & 1 & -7.433 & 0 & 2 & 0 \\ 2 & 0 & 0 & 0 & 2 & 0 & 0 & 0 & -7.433 \end{array}\right)$$

$$\left(\begin{array}{ccc|ccc|ccc} -1 & 1 & -4.455 & 1 & 1 & 0 & -2 & 0 & 0 \\ 1 & 1 & 0 & 1 & -1 & -4.455 & 0 & 5.561 & 0 \\ 5.561 & 0 & 0 & 0 & 5.561 & 0 & 0 & 0 & 3.107 \end{array}\right)$$

$$\left(\begin{array}{ccc|ccc|ccc} -1 & 1 & 1.424 & 1 & 1 & 0 & -1.166 & 0 & 0 \\ 1 & 1 & 0 & 1 & -1 & 1.424 & 0 & -1.166 & 0 \\ 3.391 & 0 & 0 & 0 & 3.391 & 0 & 0 & 0 & -3.448 \end{array}\right)$$

$$\left(\begin{array}{ccc|ccc|ccc} -14.069 & 14.069 & 2.678 & 14.069 & 14.069 & 0 & 31.806 & 0 & 0 \\ 14.069 & 14.069 & 0 & 14.069 & -14.069 & 2.678 & 0 & 31.806 & 0 \\ -4.84 & 0 & 0 & 0 & -4.84 & 0 & 0 & 0 & -1 \end{array}\right)$$

A.2 Mn_3Ge

Spin conductivity components allowed by the magnetic point group of Mn_3Ge. The matrices separated by the vertical lines represent the components of the spin conductivity polarized along x, y, z directions in the Cartesian basis, with y axis coinciding with the crystal $\vec{b}$ direction, and z axis coinciding with the crystal $\vec{c}$ direction.

$$\left(\begin{array}{ccc|ccc|ccc} 0 & 0 & 0 & 0 & 0 & 0 & 0 & 0 & 0 \\ 0 & 0 & 0 & 0 & 0 & 0 & 0 & 0 & 0 \\ 0 & 0 & 1 & 0 & 0 & -1.366 & 0 & 0 & 0 \end{array}\right)$$

$$\left(\begin{array}{ccc|ccc|ccc} 0 & 0 & 0 & 0 & -1.732 & 0 & 0 & 0 & 0 \\ 2 & -1 & 0 & -1 & 1.366 & 0 & 0 & 0 & 0 \\ 0 & 0 & 0 & 0 & 0 & 0 & 0 & 0 & 0 \end{array}\right)$$

$$\left(\begin{array}{ccc|ccc|ccc} 10.644 & -46.546 & 0 & 10.644 & -2.803 & 0 & 0 & 0 & 0 \\ 15.570 & -1.000 & 0 & 19.933 & -11.226 & 0 & 0 & 0 & 0 \\ 0 & 0 & 0 & 0 & 0 & 0 & 0 & 0 & 0 \end{array}\right)$$

$$\left(\begin{array}{ccc|ccc|ccc} 12.913 & 1.000 & 0 & -10.812 & 6.215 & 0 & 0 & 0 & 0 \\ -11.695 & 5.891 & 0 & 1.568 & -11.461 & 0 & 0 & 0 & 0 \\ 0 & 0 & 0 & 0 & 0 & 0 & 0 & 0 & 0 \end{array}\right)$$

$$\left(\begin{array}{ccc|ccc|ccc} -12.061 & 1.000 & 0 & -7.311 & 6.025 & 0 & 0 & 0 & 0 \\ 6.199 & 10.970 & 0 & 7.928 & -3.092 & 0 & 0 & 0 & 0 \\ 0 & 0 & 0 & 0 & 0 & 0 & 0 & 0 & 0 \end{array}\right)$$

$$\left(\begin{array}{ccc|ccc|ccc} 0 & 0 & 0 & 0 & 0 & 0 & 0 & 0 & 0 \\ 0 & 0 & 0 & 0 & 0 & 0 & 0 & 0 & 0 \\ 0 & 0 & 0 & 0 & 0 & 0 & -1 & 1.366 & 0 \end{array}\right)$$

$$\left(\begin{array}{ccc|ccc|ccc} 0 & 0 & 0 & 0 & 0 & 0 & 0 & 0 & 1 \\ 0 & 0 & 0 & 0 & 0 & 0 & 0 & 0 & -1.366 \\ 0 & 0 & 0 & 0 & 0 & 0 & 0 & 0 & 0 \end{array}\right)$$

A.3 Mn_3Sn

Spin conductivity components allowed by the magnetic point group of Mn_3Ge. The basis convention is the same as for Mn_3Ge.

$$\left(\begin{array}{ccc|ccc|ccc} 0 & 0 & 0 & 0 & 0 & 0 & 0 & 0 & 0 \\ 0 & 0 & 0 & 0 & 1 & 0 & 0 & 0 & 0 \\ 0 & 0 & 0 & 0 & 0 & 0 & 0 & 0 & 0 \end{array}\right)$$

$$\left(\begin{array}{ccc|ccc|ccc} 0 & 0 & 0 & 0 & -1.732 & 0 & 0 & 0 & 0 \\ 2 & -1 & 0 & -1 & 1.366 & 0 & 0 & 0 & 0 \\ 0 & 0 & 0 & 0 & 0 & 0 & 0 & 0 & 0 \end{array}\right)$$

$$\left(\begin{array}{ccc|ccc|ccc} 0 & 0 & 0 & 0 & 0 & 0 & 0 & 0 & 0 \\ 0 & 0 & 0 & 0 & 0 & 0 & 0 & 0 & 1 \\ 0 & 0 & 0 & 0 & 0 & 0 & 0 & 0 & 0 \end{array}\right)$$

$$\left(\begin{array}{ccc|ccc|ccc} 0 & 0 & 0 & 0 & 0 & 0 & 0 & 0 & 0 \\ 16.513 & -1.106 & 0 & -1.106 & 1 & 0 & 0 & 0 & 0 \\ 0 & 0 & 0 & 0 & 0 & 0 & 0 & 0 & 0 \end{array}\right)$$

$$\left(\begin{array}{ccc|ccc|ccc} 0 & 0 & 0 & 0 & 0 & 0 & 0 & 0 & 0 \\ 0 & 0 & 0 & 0 & 0 & 0 & 0 & 0 & 1 \\ 0 & 0 & 0 & 0 & 0 & 0 & 0 & 0 & 0 \end{array}\right)$$

$$\left(\begin{array}{ccc|ccc|ccc} 0 & 0 & 0 & 14.928 & -1 & 0 & 0 & 0 & 0 \\ 0 & 0 & 0 & -1 & -2.732 & 0 & 0 & 0 & 0 \\ 0 & 0 & 0 & 0 & 0 & 0 & 0 & 0 & 0 \end{array}\right)$$

$$\left(\begin{array}{ccc|ccc|ccc} 0 & 0 & 0 & 0 & 0 & 0 & 0 & 0 & 0 \\ 0 & 0 & 0 & 0 & 0 & 0 & 0 & 0 & 0 \\ 0 & 0 & 0 & 0 & 0 & 0 & 0 & 1 & 0 \end{array}\right)$$

A.4 Mn_3NiN

Spin conductivity components allowed by the magnetic point group of Mn_3NiN, presented in a Cartesian basis. Similarly to Mn_3Ir, the basis is rotated such that the allowed weak ferromagnetic moment is oriented in the z direction. The allowed tensor components also share a special form, especially for σ^3_{ij}, polarized in the direction of the weak ferromagnetic moment.

$$\left(\begin{array}{ccc|ccc|ccc} 3.391 & 2.652 & -6.044 & 2.653 & -3.392 & 0.737 & 1.403 & 0 & 0 \\ 2.652 & -3.391 & -0.738 & -3.392 & -2.653 & -6.044 & 0 & 1.403 & 0 \\ -6.044 & -0.738 & 0 & 0.737 & -6.044 & 0 & 0 & 0 & 1.403 \end{array}\right)$$

$$\left(\begin{array}{ccc|ccc|ccc} -2.156 & 5.274 & 2.419 & 5.274 & 2.156 & -5.077 & 2.825 & 0.692 & 0 \\ 5.274 & 2.157 & 5.077 & 2.157 & -5.274 & 2.418 & -0.693 & 2.825 & 0 \\ -2.387 & 1.460 & 0 & -1.461 & -2.388 & 0 & 0 & 0 & 1.625 \end{array}\right)$$

$$\left(\begin{array}{ccc|ccc|ccc} 0.818 & 2.468 & -4.663 & 2.469 & -0.818 & 2.640 & -3.382 & -0.809 & 0 \\ 2.468 & -0.818 & -2.640 & -0.818 & -2.468 & -4.663 & 0.809 & -3.381 & 0 \\ 7.174 & -2.160 & 0 & 2.160 & 7.174 & 0 & 0 & 0 & -2.725 \end{array}\right)$$

$$\left(\begin{array}{ccc|ccc|ccc} -0.214 & -1.462 & 1.165 & -1.462 & 0.214 & -8.237 & -1.300 & 2.106 & 0 \\ -1.461 & 0.214 & 8.237 & 0.214 & 1.462 & 1.165 & -2.106 & -1.300 & 0 \\ -3.389 & -4.778 & 0 & 4.778 & -3.389 & 0 & 0 & 0 & -0.574 \end{array}\right)$$

$$\left(\begin{array}{ccc|ccc|ccc} 1.926 & -2.428 & -4.177 & -2.430 & -1.926 & -5.591 & 2.869 & 1.001 & 0 \\ -2.428 & -1.926 & 5.591 & -1.926 & 2.429 & -4.177 & -1.001 & 2.869 & 0 \\ 2.452 & 5.503 & 0 & -5.502 & 2.453 & 0 & 0 & 0 & 1.201 \end{array}\right)$$

$$\left(\begin{array}{ccc|ccc|ccc} 2.361 & -1.474 & 3.021 & -1.474 & -2.361 & -0.413 & -6.801 & -4.167 & 0 \\ -1.473 & -2.362 & 0.413 & -2.361 & 1.474 & 3.021 & 4.168 & -6.800 & 0 \\ -4.366 & 2.537 & 0 & -2.537 & -4.365 & 0 & 0 & 0 & 0.745 \end{array}\right)$$

$$\left(\begin{array}{ccc|ccc|ccc} 2.308 & -1.053 & 2.843 & -1.053 & -2.308 & 0.301 & -5.795 & 0.249 & 0 \\ -1.053 & -2.309 & -0.301 & -2.308 & 1.053 & 2.843 & -0.249 & -5.795 & 0 \\ -0.918 & 0.794 & 0 & -0.794 & -0.918 & 0 & 0 & 0 & 10.771 \end{array}\right)$$

$$\left(\begin{array}{ccc|ccc|ccc} -0.279 & 0.850 & -1.480 & 0.849 & 0.279 & -0.200 & -4.711 & 8.744 & 0 \\ 0.849 & 0.278 & 0.200 & 0.278 & -0.850 & -1.480 & -8.744 & -4.711 & 0 \\ -1.459 & 1.437 & 0 & -1.437 & -1.459 & 0 & 0 & 0 & -3.874 \end{array}\right)$$

$$\left(\begin{array}{ccc|ccc|ccc} 4.804 & 1.886 & 2.910 & 1.886 & -4.803 & -2.891 & -0.032 & 3.879 & 0 \\ 1.886 & -4.804 & 2.891 & -4.803 & -1.886 & 2.911 & -3.879 & -0.031 & 0 \\ 2.693 & -3.550 & 0 & 3.550 & 2.694 & 0 & 0 & 0 & -4.284 \end{array}\right)$$

B Code

The code used in calculations is available in the following GitHub repository: https://github.com/sjpolak/Project-Altermagnetism

C AI statement

In this project, ChatGPT and Deepseek R1 were used for generating parts of the code, typesetting complex LaTeX expressions, and screening for mistakes in the paper.